Novel electronic wave interference patterns in nanographene sheets

Kikuo Harigaya†‡§‖, Yousuke Kobayashi§, Kazuyuki Takai§, Jérôme Ravier§, and Toshiaki Enoki§

†Nanotechnology Research Institute, AIST, Tsukuba 305-8568, Japan
‡Synthetic Nano-Function Materials Project, AIST, Tsukuba 305-8568, Japan
§Tokyo Institute of Technology, Oh-okayama, Meguro-ku 152-8551, Japan

Abstract. Superperiodic patterns with a long distance in a nanographene sheet observed by STM are discussed in terms of the interference of electronic wave functions. The period and the amplitude of the oscillations decrease spatially in one direction. We explain the superperiodic patterns with a static linear potential theoretically. In the $\boldsymbol{k} \cdot \boldsymbol{p}$ model, the oscillation period decreases, and agrees with experiments. The spatial difference of the static potential is estimated as 1.3 eV for 200 nm in distance, and this value seems to be natural. It turns out that the long-distance oscillations come from the band structure of the two-dimensional graphene sheet.

1. Introduction

Nanographene sheets are attractive materials, because their magnetic and transport properties show novel and peculiar properties, originating from nonbonding states localized at the zigzag-edges [1,2]. Theoretical works [2-5] have been performed to clarify the mechanisms of the unique magnetism. It has been found that the A-B stacking and the presence of the localized electronic spins originating in the open shell nature are the favorable conditions for the magnetism.

On the other hand, direct observation by scanning tunneling microscope (STM) is powerful for structural analysis as well as for investigation of electronic properties. Previously, we have reported that the interlayer distance of a single nanographene on a highly oriented pyrolytic graphite (HOPG) substrate is about 0.35-0.37 nm and is larger than that of bulk material [6]. In recent study, we have found superperiodic patterns with extremely long periodicity in the STM images of a nanographene sheet, which varies spatially [7]. In this paper, we give an explanation for this novel results in terms of the interference of electronic wave functions.

In order to understand the origins of the long-distance oscillations which were observed, we will make a comparison with the theoretical electron densities using the free electron model confined within an infinite square well, and also using the $\boldsymbol{k} \cdot \boldsymbol{p}$ model [8,9] for two-dimensional graphene sheet. One of the present authors has used the model for the understandings of the multi channel Kondo effect [10] and the Cooper pair propagation [11] in metallic carbon nanotubes. In the graphene sheets, superperiodic patterns in STM images due to the moiré origins for the A-B stacking

‖ To whom correspondence should be addressed (E-mail: k.harigaya@aist.go.jp, URL: http://staff.aist.go.jp/k.harigaya/)
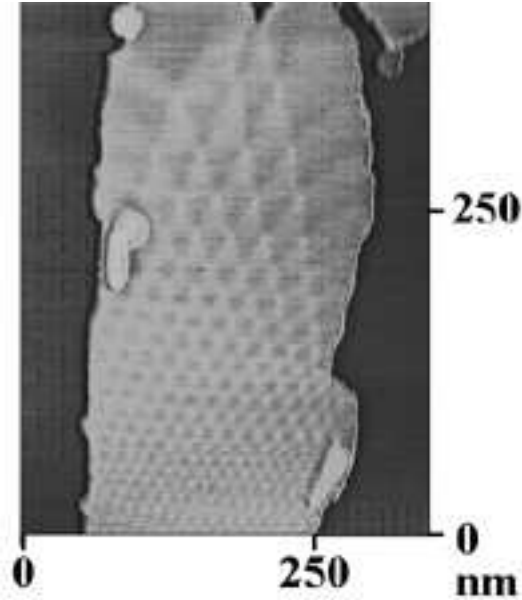
Figure 1. STM image of the superperiodic pattern on a necktie-shaped graphene plate on HOPG substrate.

[12] and structural deformations [13] have been reported in the literatures. However, the observed superperiodic patterns with quite long periods over 10 nm seem not coming from the moiré mechanism, and our finding calls for new interpretations. We assume the presence of a static potential with a linear decrease in one direction. The calculated local electron density will be compared with the experiments. We will clarify that the long-distance oscillations are due to the presence of electrons with the band structure of a two-dimensional graphene sheet.

This paper is organized as follows. In section 2, the experimental results are briefly reviewed. In section 3, calculations by the free electron model are compared with experiments. In section 4, the analysis with the $\boldsymbol{k} \cdot \boldsymbol{p}$ model is performed. The paper is closed with summary in section 5.

2. STM observations

In this section, the experimental data is briefly reviewed. In Fig. 1, a STM image of the graphene sheet with a necktie shape is shown. The detail will be published elsewhere. The observation has been done with the following condition: bias voltage V = 200 mV and current I = 0.7 nA. The distance between the graphene necktie and the substrate is over 0.8 nm, suggesting that it consists of a stacking of two graphene layers, which interact weekly with the HOPG substrate. Interestingly, the period and the amplitude of the oscillations decrease from the top to the bottom along the graphene necktie. The oscillation period is one order of magnitude larger than that of the moiré pattern due to stacking [12], and therefore this possibility can be excluded. We can assume effects of long-distance periodic-structural deformations [13] in the graphene surface or interference effects of electronic wave functions.

We have also observed that the oscillation period becomes longer by placing a nanographene flake on the graphene necktie, as shown in Fig. 2. The oscillations period seems to be double in the upper region of the necktie after addition of one flake. The
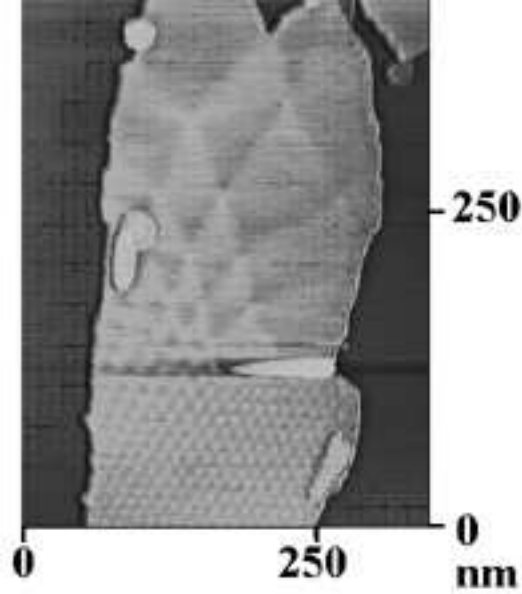
Figure 2. STM image of the superperoidic pattern on the necktie-shaped graphene sheet observed in Fig. 1 after a nanographene flake is placed.

oscillation below the flake seems to be only slightly modified by the flake. Such effect on the oscillations cannot be explained by some structural modulations. Therefore, the oscillation patterns could be the effect of interference of the electronic wave functions in the graphene surface.

3. Free electron model

We will characterize the interference patterns theoretically. Two dimensional coordinate is defined so that the y-axis is along with the long direction of the graphene necktie. The x-axis is perpendicular to the y-axis. By assuming the electric static potential $-F \cdot y$ which is proportional to the y-axis, and the confinement effect due to the well-shaped potential within $-d/2 < x < d/2$, we obtain the Schrödinger equation:

$$\left[-\frac{\hbar^2}{2m} \left(\frac{\partial^2}{\partial x^2} + \frac{\partial^2}{\partial y^2} \right) + V_{\text{well}}(x) - F \cdot y \right] \psi(x,y) = E\psi(x,y), \tag{1}$$

where $V_{\text{well}}(x)$ means the well potential with the infinite depth. The electron density with the energy E is written as:

$$|\psi(x,y)|^2 = \sum_n a_n |\psi_x(E_n)\psi_y(E - E_n)|^2, \tag{2}$$

where a_n is the coefficient of the occupancy with the quantum number n, $\psi_x(E_n)$ is the solution in the well in the x-direction, and $\psi_y(E - E_n)$ is the solution for the potential term $-F \cdot y$. The solution in the well is:

$$\psi_x(E_n) = \begin{cases} A\cos\left(\frac{n\pi x}{d}\right) \text{ for odd } n \\ A\sin\left(\frac{n\pi x}{d}\right) \text{ for even } n \end{cases}, \tag{3}$$
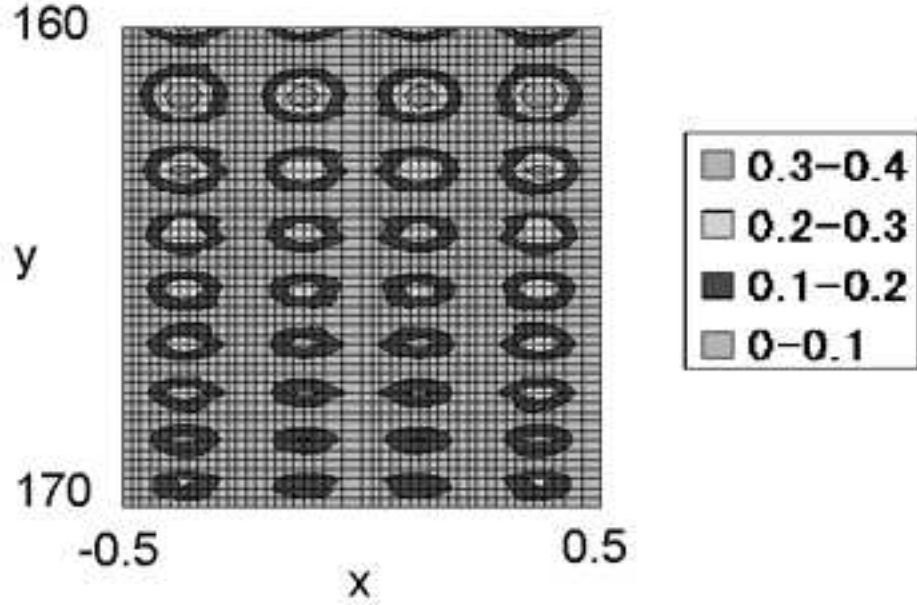
Figure 3. Two dimensional plot of the electron density calculated by the free electron model. The bottom and left axes are shown in arbitrary units. The quantum number $n = 4$ is taken for the standing wave within the infinite well, $-0.5 < x < 0.5$ with $d = 1$.

with $E_n = \pi^2 \hbar^2 n^2 / 2md^2$ and $A = \sqrt{2/d}$. The solution for the linear potential is:

$$\psi_y(E - E_n) = \Phi\left[-\left(\frac{2mF}{\hbar^2}\right)^{1/3}\left(x + \frac{E}{F} - \frac{E_n}{F}\right)\right], \tag{4}$$

where $\Phi(x)$ is the Airy function

$$\Phi(x) = \frac{1}{\sqrt{\pi}} \int_0^\infty \cos\left(\frac{u^3}{3} + ux\right) \mathrm{d}u. \tag{5}$$

The local density of states of electrons with $a_n = 1$ only for $n = 4$ is shown in Fig. 3. We can theoretically explain the decrease of the oscillation period and the amplitude along the y-direction. This property is owing to the form of the Airy function. There is a standing wave in the x-direction. However, we cannot explain the details of oscillations in the x-direction of Fig. 1, possibly by the effects of the complex shapes of the boundary in the graphene necktie.

Even though the oscillation in the well is uniform spatially, we can compare the oscillation patterns in the y-direction at least. Figure 4 shows comparison with the experiment where the peak positions along the long axis of the necktie are plotted. The decrease of the amplitude of the theoretical curve seems more rapid than that of the experimental data. The strength of the static potential is $F = 5.26 \times 10^{-6}$ eV/nm with using the free electron mass. The potential variation over the distance 200 nm is 1.1×10^{-3} eV, and this is quite small. Phonon fluctuation effects or the presence of impurities can override such the small potential change. This difficulty might be due to the assumption of the free electron model of this section.
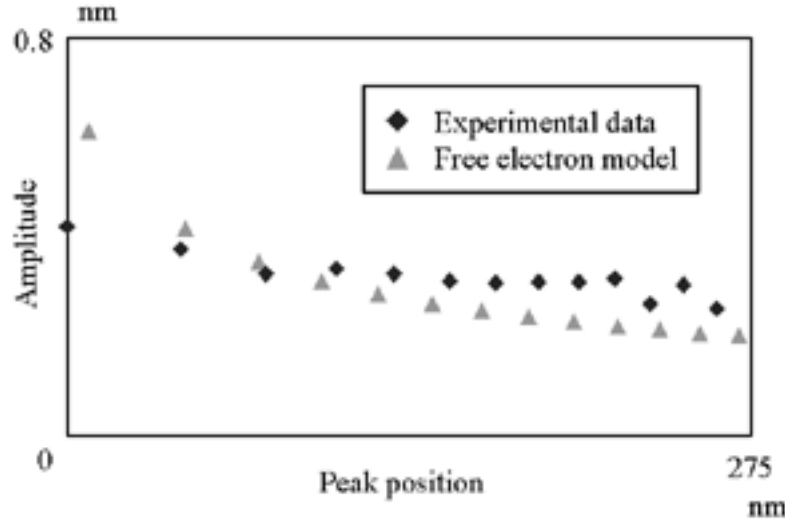
Figure 4. Comparison for the electron wave patterns by STM and the free electron theory. Experimental peak positions along the perpendicular direction of Fig. 1 are plotted by diamonds. The results of the fitting by one dimensional free electron model are shown by triangles.

4. Continuum $\boldsymbol{k} \cdot \boldsymbol{p}$ model

In order to substantiate analysis of the interference patterns, we give comparison with the calculation of the model for the graphene plane. Here, we use the continuum $\boldsymbol{k} \cdot \boldsymbol{p}$ model [7,8]. The hamiltonian around the K point with the linear potential $-F \cdot y$ is:

$$
H = \begin{pmatrix} -F \cdot y & -i\gamma\frac{\partial}{\partial x} - \gamma\frac{\partial}{\partial y} \\ -i\gamma\frac{\partial}{\partial x} + \gamma\frac{\partial}{\partial y} & -F \cdot y \end{pmatrix},
\tag{6}
$$

where $\gamma \equiv (\sqrt{3}/2)a\gamma_0$, a is the bond length, and γ_0 is the hopping integral between neighboring carbon atoms. This model is solved together with the infinite well potential $V_{\text{well}}(x)$ as used in the previous section. The Schrödinger equation $H\Psi = E\Psi$ gives a oscillating solution:

$$
\Psi = 2A \begin{pmatrix} \sin\left(\frac{E_n x}{\gamma}\right) \\ -i\cos\left(\frac{E_n x}{\gamma}\right) \end{pmatrix} \otimes \begin{pmatrix} \sin\left[\frac{1}{\gamma}\left(\tilde{E}y + \frac{1}{2}Fy^2\right)\right] \\ \cos\left[\frac{1}{\gamma}\left(\tilde{E}y + \frac{1}{2}Fy^2\right)\right] \end{pmatrix},
\tag{7}
$$

where $E_n = n\pi\gamma/d$ and $\tilde{E} = E - E_n$. The electron density at the A-sublattice point is calculated as:

$$
|\psi_A(\boldsymbol{R}_A)|^2 = 4A^2\sin^2\left(\frac{n\pi x}{d}\right)
$$
$$
\times \left\{1 + \cos[(\boldsymbol{K} - \boldsymbol{K'}) \cdot \boldsymbol{R}_A]\sin\left[\frac{2}{\gamma}\left(\tilde{E}y + \frac{1}{2}Fy^2\right)\right]\right\}
\tag{8}
$$

where $\boldsymbol{R}_A$ is the lattice point of the A-sublattice, $\boldsymbol{K}$ and $\boldsymbol{K'}$ are the K and K' points in the wave number space. We pay attention to the long period oscillating component:

$$
\sin^2\left(\frac{n\pi x}{d}\right)\left[\text{const.} + \sin\left(\frac{Fy^2}{\gamma} - \frac{2n\pi}{d}y\right)\right],
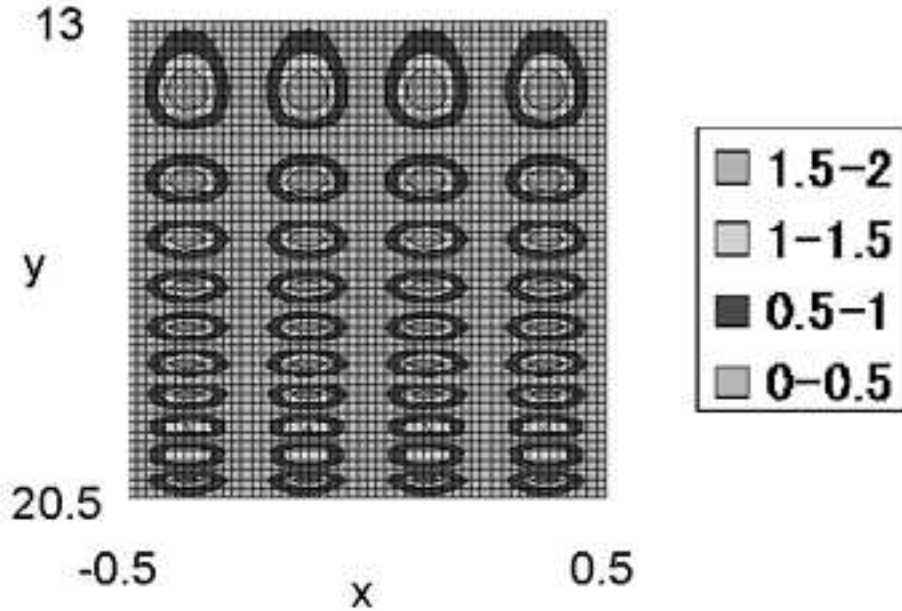\tag{9}
$$

Figure 5. Two dimensional plot of the electron density calculated by the $\boldsymbol{k} \cdot \boldsymbol{p}$ model. The bottom and left axes are shown in arbitrary units. The quantum number $n = 4$ is taken for the standing wave within the infinite well, $-0.5 < x < 0.5$ with $d = 1$.

where we take $E = 0$ at the Fermi energy. This functional form for the quantum number $n = 4$ is plotted in Fig. 5 with the assumption $d = 1$. The amplitude is spatially constant, and the oscillation period becomes smaller as y becomes larger. We can explain the decrease of the oscillation period found in experiments of Fig. 1, though the uniform array of the standing wave would be the result of the simplified theory and this is in contrast with the observations.

The peak positions of the electron density in the long direction of the graphene necktie of Fig. 1 are plotted in Fig. 6, and comparison with the result of eq. (9) is given. The slight decrease found in the experiments cannot be reproduced by the result of the $\boldsymbol{k} \cdot \boldsymbol{p}$ model. However, the decrease of the oscillation period fairly agrees with the experiments. The fitting gives the parameter of the potential gradient $F = 6.49 \times 10^{-3}$ eV/nm. The total potential variation over the distance 200 nm becomes 1.3 eV. Such magnitude of the potential change would survive thermal lattice fluctuations and can really exist in experiments. The present result by no means implies that the wave functions observed with superperiodic amplitudes are of the electrons which have energy levels of the graphene plane.

5. Summary

Superperiodic patterns in a nanographene sheet observed by STM can be explained with two models of electronic wave functions in terms of the interference. First, the experimental results have been briefly introduced. The period and the amplitude of the oscillations decrease spatially in one direction along with the long direction of the graphene necktie. The patterns are superperiodic, and the period is one order of the magnitudes longer than that of the well known moiré pattern observed in A-B stacked graphite systems. This is a novel finding in our experiments.
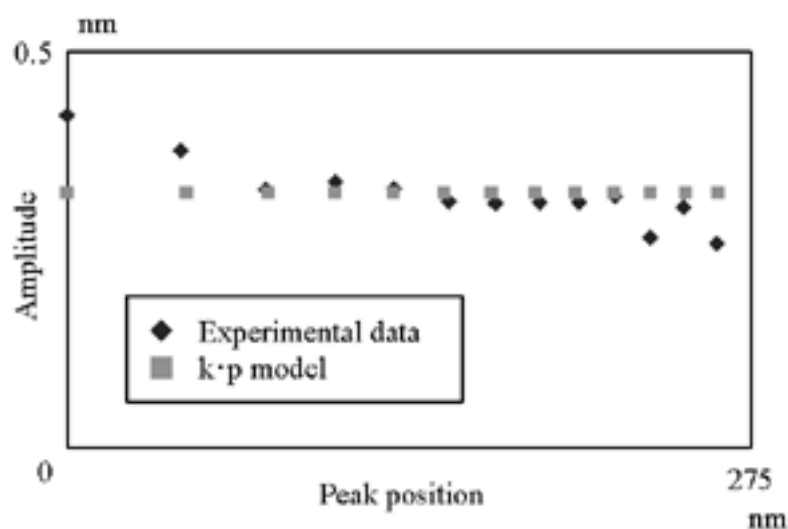
Figure 6. Comparison for the electron wave patterns by STM and the $\boldsymbol{k} \cdot \boldsymbol{p}$ model. Experimental peak positions along the perpendicular direction of Fig. 1 are plotted by diamonds. The results of the fitting by the long distance envelope functional form derived from the $\boldsymbol{k} \cdot \boldsymbol{p}$ model are shown by squares.

Next, theoretical characterizations have been reported. We have explained the interference patterns with the static linear potential by using a free electron model and also by the continuum $\boldsymbol{k} \cdot \boldsymbol{p}$ model. In the free electron model, we have derived the decrease of the oscillation period and the amplitude along the decreasing direction of the linear potential. However, the strength of the linear potential turned out to be unrealistically too small. In the $\boldsymbol{k} \cdot \boldsymbol{p}$ case, the oscillation period decreases, and the amplitude is constant. The spatial difference of the static potential is estimated as 1.3 eV for the distance 200 nm, and this value seems to be natural. It turned out that the long distance oscillations come from electrons with the band structures of the two dimensional graphene sheet.

Acknowledgements

References

[1] Y. Shibayama, H. Sato, T. Enoki, and M. Endo, Phys. Rev. Lett. **84**, 1744 (2000).
[2] K. Harigaya and T. Enoki, Chem. Phys. Lett. **351**, 128 (2002).
[3] K. Harigaya, N. Kawatsu, and T. Enoki, in "Nanonetwork Materials: Fullerenes, Nanotubes, and Related Systems", (American Institute of Physics, 2001), pp. 529-532.
[4] K. Harigaya, J. Phys.: Condens. Matter **13**, 1295 (2001).
[5] K. Harigaya, Chem. Phys. Lett. **340**, 123 (2001).

[6] A. M. Affoune, B. L. V. Prasad, H. Sato, T. Enoki, Y. Kaburagi, and Y. Hishiyama, Chem. Phys. Lett. **348**, 17 (2001).

[7] Y. Kobayashi, K. Takai, J. Ravier, T. Enoki, and K. Harigaya, (unpublished results).

[8] H. Ajiki and T. Ando, J. Phys. Soc. Jpn. **62**, 1255 (1993).

[9] T. Ando and T. Nakanishi, J. Phys. Soc. Jpn. **67**, 1704 (1998).

[10] K. Harigaya, New J. Phys. **2**, 9 (2000).

[11] K. Harigaya, J. Phys.: Condens. Matter **12**, 7069 (2000).

[12] K. Kobayashi, Phys. Rev. B **53**, 11091 (1996).

[13] T. M. Bernhardt, B. Kaiser, and K. Rademann, Surface Science **408**, 86 (1998).